

Structure of low-coverage phases of Al, Ga, and In on Si(100)

John E. Northrup and M. C. Schabel

Xerox Palo Alto Research Center, 3333 Coyote Hill Road, Palo Alto, California 94304

C. J. Karlsson and R. I. G. Uhrberg

Department of Physics and Measurement Technology, Linköping Institute of Technology, S-581 83 Linköping, Sweden

(Received 22 August 1991)

The atomic structures of the low-coverage 2×2 phases of Al, Ga, and In on Si(100) were determined on the basis of first-principles total-energy calculations and angle-resolved photoemission experiments. The proposed structure consists of rows of ad-dimers, with the ad-dimers oriented parallel to the underlying Si dimers. Angle-resolved photoemission experiments performed for Si(100) 2×2 :In are in good agreement with the calculated surface-state dispersions for the parallel ad-dimer model. The existence of lower coverage 3×2 and 5×2 phases results from repulsive interactions between neighboring rows of ad-dimers.

The adsorption of Al, Ga, and In on the Si(100) surface leads to the formation of several well-ordered phases having coverages of less than one monolayer. Although low-energy-electron-diffraction (LEED) and scanning-tunneling-microscopy (STM) studies have provided much information about these systems, the local atomic structure has not yet been established. In this paper we report a determination of the structure of the 2×2 phase based on first-principles total-energy calculations. We have also performed angle-resolved photoemission experiments for Si(100) 2×2 :In, and comparisons between the experimental data and calculated surface-state dispersions strongly support the structure obtained from energy minimization.

Reflection high-energy electron-diffraction experiments due to Sakamoto and Kawanami¹ established the existence of phases with 3×2 , 5×2 , 2×2 , and 8×1 symmetry for Ga coverages less than one monolayer and temperatures between 350°C and 680°C. More recently, Bourguignon, Carleton, and Leone² examined the evolution of the first monolayer of Ga on Si(100) with LEED and also observed these ordered structures. In addition, they reported a 2×1 phase at 1 monolayer of Ga. They concluded that the 2×2 structure has a coverage of $\frac{1}{2}$ monolayer and results in the complete saturation of the dangling bonds of the dimerized Si(100) substrate. Their results also indicated that the Si-Ga bonding changes qualitatively for coverages greater than $\frac{1}{2}$ monolayer. The structural model suggested by these authors for the 2×2 phase is indicated in Fig. 1(a). It consists of a metal ad-dimer adsorbed between the Si dimer rows: the ad-dimer is oriented orthogonally to the Si-Si dimer bond. Rows of these ad-dimers can be arranged with various inter-row spacings to form structures with 3×2 and 5×2 symmetry. Aluminum-induced 2×2 and 3×2 phases have also been observed with LEED.³

STM studies due to Nogami and co-workers⁴⁻⁸ have shown that Al, Ga, and In initially grow in the form of long rows. The rows grow fastest along the $2 \times$ direction of the underlying dimerized Si surface. This growth mode continues until the 2×2 structure is completed at $\frac{1}{2}$ monolayer. These studies indicate that the formation of

the 2×2 structure occurs without the disruption of the underlying Si-Si dimer bond. These authors noted that in addition to the orthogonal ad-dimer model, the parallel ad-dimer model was also consistent with their STM images. This model is illustrated in Fig. 1(b).

Up to now, there has been no experimental or theoretical evidence which distinguishes between the parallel and orthogonal ad-dimer models. The first-principles total-energy calculations reported here strongly favor the paral-

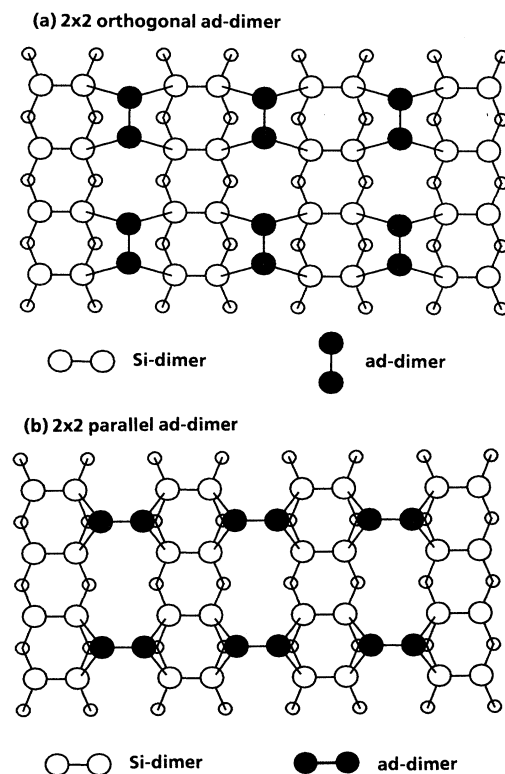


FIG. 1. (a) Top view of Si(100) 2×2 orthogonal ad-dimer structure. (b) Si(100) 2×2 parallel ad-dimer structure.

lel ad-dimer model. Moreover, we find that the surface-state spectrum calculated on the basis of the parallel ad-dimer model is in good agreement with angle-resolved photoemission data for the Si(100)2×2:In surface.

The total energy and force calculations^{9,10} were performed within the local-density approximation,¹¹ and employed scalar relativistic pseudopotentials.¹² The surface geometry was represented by a 10-layer slab of Si with adsorbates on each side of the slab. A plane-wave cutoff of 10 Ry was employed. To allow energetic comparisons involving structures with different coverages we calculate the chemical-potential-dependent formation energy:

$$\Omega(\mu_{\text{ad}}) = E - n_{\text{Si}}\mu_{\text{Si}(\text{bulk})} - n_{\text{ad}}\mu_{\text{ad}}.$$

Under equilibrium conditions, the maximum possible value for μ_{ad} is equal to the chemical potential of the bulk phase of the adsorbate. This approach allows comparison of the 2×2 ad-dimer structures having $\frac{1}{2}$ monolayer coverage with the 2×1 dimer structure having 1 monolayer coverage. The relative energy of the parallel and orthogonal ad-dimer model is, of course, independent of the chemical potential of the adsorbate.

The total-energy calculations strongly favor the parallel ad-dimer model over the orthogonal ad-dimer model for Al, Ga, and In ad-dimers. For In, the surface energy of the parallel ad-dimer is found to be 0.23 eV/(1×1) lower than the orthogonal ad-dimer. This energy difference is quite well converged with respect to plane-wave cutoff: reducing the energy cutoff from 10 to 7 Ry changed this energy difference by less than 0.01 eV/(1×1). For Ga the surface energy for the parallel ad-dimer is 0.33 eV/(1×1) lower than the orthogonal ad-dimer. For Al the parallel ad-dimer model is lower by 0.33 eV/(1×1). These energy differences are quite significant: the energy difference per ad-dimer is 0.92 eV for In and 1.32 eV for Al and Ga. In a previous theoretical study by Batra,¹³ the lowest-energy 2×2 structure obtained was an orthogonal Al-Al dimer on an ideal Si(100) substrate. The parallel ad-dimer model was not considered in that study.

The calculated Si-Si and ad-dimer bond lengths for the 2×2 structures are given in Table I. It is significant that both the Si-atom bond length and the Si-Si dimer bond length are closer to the sum of the Pauling covalent radii in the parallel ad-dimer model than in the orthogonal ad-dimer model. This accounts for the much greater stability of the parallel ad-dimer structure. In the orthogonal

TABLE I. Calculated bond lengths (in Å). For covalent bonding one expects bond lengths approximately equal to the sum of the Pauling covalent radii. The radii are 1.17 Å for Si, 1.27 Å for Al and Ga, and 1.44 Å for In. Δz is the separation between the planes containing the ad-dimers and the Si dimers.

	Si(100)2×2:Al		Si(100)2×2:Ga		Si(100)2×2:In	
	Para	Ortho	Para	Ortho	Para	Ortho
Si-Si dimer	2.44	2.69	2.46	2.84	2.40	2.61
ad-dimer	2.69	2.58	2.63	2.50	2.82	2.76
Si-atom	2.47	2.67	2.47	2.61	2.60	2.74
Δz	1.10	0.71	1.09	0.73	1.38	0.91

ad-dimer configuration the Si-Si dimer bond is highly strained.

Calculations were also performed for the 2×1 surfaces having one monolayer of In or Ga dimers. These surfaces may be obtained by replacing the Si-Si dimers of the Si(100)2×1 surface within In-In dimers. The energies of these surfaces may be compared with those of the 2×2 surfaces as a function of the adsorbate chemical potential. The results for In are shown in Fig. 2(a). For $\mu_{\text{In}} < \mu_{\text{In}(\text{bulk})}$ the 2×2 ad-dimer structure has a significantly lower surface energy than the 2×1. Thus a 2×1 In-dimer structure would not occur under equilibrium conditions. The corresponding results for Ga are shown in Fig. 2(b). For Ga, the 2×1 dimer structure becomes competitive with the 2×2 structure for μ_{Ga} slightly larger than the chemical potential of the bulk. According to these results the stability of the 2×1 Ga-dimer structure with respect

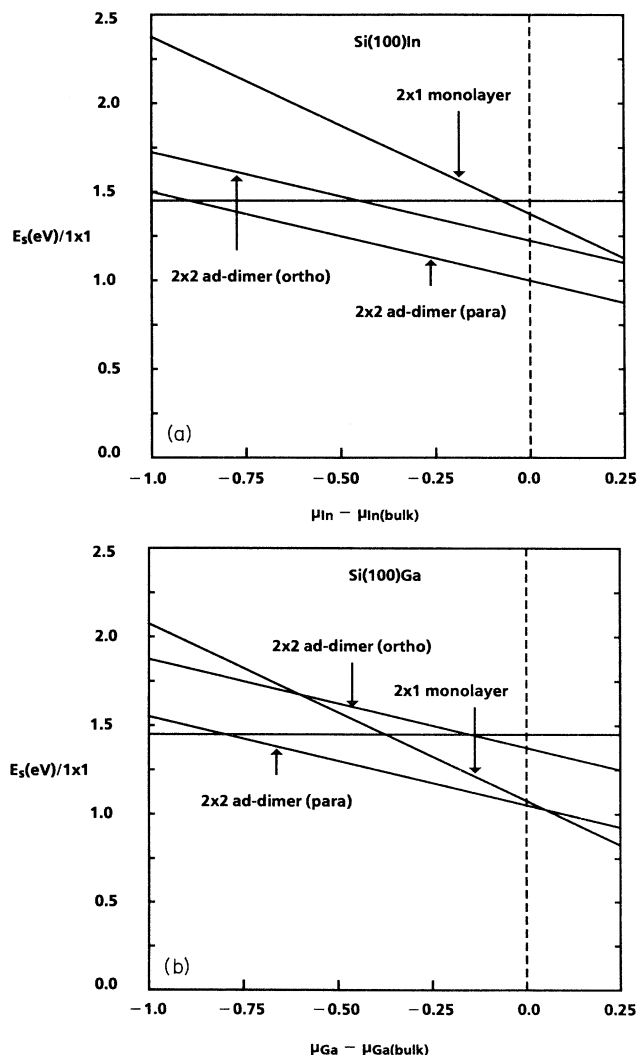


FIG. 2. (a) Chemical-potential-dependent surface formation energies for the Si(100)2×2:In and Si(100)2×1:In surfaces discussed in the text. (b) Surface energies for Si(100)Ga surfaces. The surface energy of the clean 2×1 surface is 1.45 eV/(1×1).

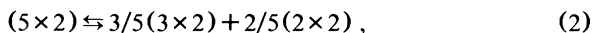
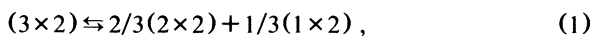
to the 2×2 requires that μ_{Ga} be at least 0.05 eV above $\mu_{\text{Ga(bulk)}}$. While this result indicates that the 2×1 Ga-dimer structure could form only under nonequilibrium conditions, we suggest that such conditions could prevail when the average Ga coverage is ~ 1 monolayer but before large Ga clusters have formed. The surface energy of a cluster gives rise to a nucleation barrier,¹⁴ and in a quasiequilibrium picture, the Ga chemical potential must rise above $\mu_{\text{Ga(bulk)}}$ in the early stages of cluster formation. As evidence that kinetics plays an important role in the appearance of the 2×1 Ga-dimer phase we note that it is observed during deposition but not during desorption.²

Structural models for the 3×2 and 5×2 phases^{1,2} (with coverages of $\frac{1}{3}$ and $\frac{2}{5}$) may be obtained by increasing the spacing between the ad-dimer rows. These phases will be stable at low coverages if there exists a repulsive interaction between rows of ad-dimers. Such an interaction leads to the stability of these phases over certain ranges of μ_{ad} . We have investigated the nature of the interaction between ad-dimer rows using the classical Si potential of Stillinger and Weber.¹⁵ This potential has been employed recently to calculate the interaction energy between steps on vicinal Si(100) surfaces.^{16,17}

Rather than attempting to modify the potential or alter the parameters to better represent the energetics of the ad-dimer-Si bond, our calculations simply employed the same potential for the ad-dimer and substrate atoms. Clearly, this approach cannot provide accurate quantitative information regarding the energy associated with ad-dimer formation. However, the interactions between adjacent ad-dimer rows are mediated by the strain fields in the Si substrate. Thus, the distortions of the first few subsurface Si layers induced by the presence of the ad-dimer atoms are central in determining the qualitative aspects of long-range row-row interactions.

Simulations were performed using a periodic supercell geometry with two-sided slabs twenty atomic-layers thick representing ad-dimer geometries ranging from 2×2 to 10×2 . The atomic structure was relaxed iteratively using a conjugate gradient scheme to minimize the energy. The interaction energy of two isolated ad-dimer rows on a Si(100): 1×2 surface was determined as a function of row separation by decomposing the surface energy for periodic cells into a sum of independent contributions from neighboring ad-dimer rows. This interaction term is purely repulsive and rapidly decreases with increasing ad-dimer row separation, with essentially no contribution from rows separated by more than four Si dimers. The repulsive terms are found to be nearly additive with respect to the configuration of ad-dimer rows.

The stability of the 3×2 and 5×2 ad-dimer phases with respect to phase separation for the atom conserving reactions



was determined by comparing the relative surface energies of the single phase and segregated configurations. In both cases we find the single phase structures to be stable with respect to dissociation into a higher coverage and a lower coverage phase. The energy cost of reaction (1) is

16 meV/(2×2) and that of reaction (2) is 1.3 meV/(2×2). The observed stability is a direct consequence of the increased row-row repulsion incurred when a more densely packed surface structure is formed.

The electronic structure of the Si(100) 2×2 :In surface was studied with angle-resolved photoemission using both 21.2 and 16.85 eV resonance light. A brief description of the experimental setup has been presented elsewhere.¹⁸ The Si(100) sample was cut from an on-axis wafer ($\rho = 4-6 \text{ m}\Omega \text{ cm}$, As doped). Before insertion into the vacuum chamber it was cleaned using the etching method of Ishizaka and Shiraki.¹⁹ The thin oxide produced by the cleaning procedure was removed in vacuum by annealing at $\sim 900^\circ\text{C}$. LEED showed a sharp, two-domain, 2×1 pattern on the clean surface prepared in this way. The two-domain structure is due to the 90° difference in the orientation of the dimers on terraces separated by a single atomic-layer step. The 2×2 :In surface will exhibit the same kind of domain structure with respect to the orientation of the In-In dimers. To avoid any ambiguities due to the presence of two domains we present the experimental and calculated band structure along the [010] azimuth [see Fig. 3(a)]. The energies of the electronic states with k_{\parallel} along this azimuth are the same in each domain.

The Si(100) 2×2 :In surface was prepared by evaporating In from a tungsten filament onto the Si(100) 2×1 sur-

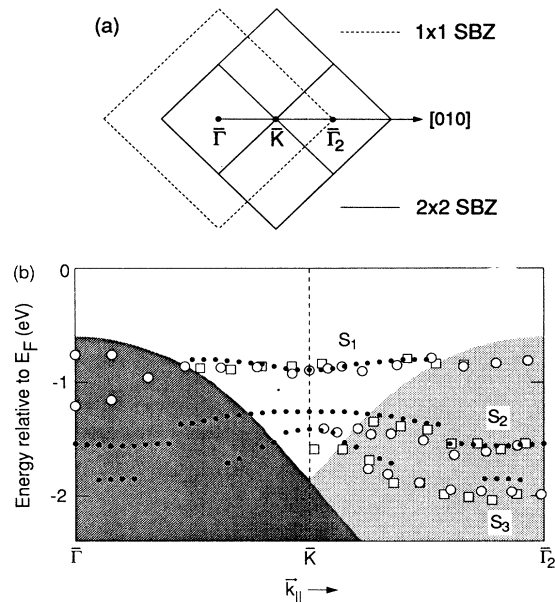


FIG. 3. (a) Surface Brillouin zones (SBZ) for a 1×1 and 2×2 reconstructed Si(100) surface. The surface electronic structure of Si(100) 2×2 :In was determined both experimentally and theoretically along the [010] direction indicated. (b) Comparison between theory (solid circles) and experimental (open symbols). The parallel ad-dimer model was employed in the calculation. Angle-resolved photoemission data were obtained with both 21.2 (open circles) and 16.85 eV (open squares) radiation. The 1×1 projected bulk band structure is shown as the dark-gray region. The lighter-gray region corresponds to the bulk band structure projected onto the 2×2 SBZ. The Fermi level was determined to be 0.6 eV above the valence-band maximum.

face at a slightly elevated temperature. At an In coverage of 0.5 monolayers, as measured by a crystal monitor, a clear 2×2 pattern was observed in LEED. Angle-resolved photoemission revealed three surface bands. The dispersion of these bands is indicated in Fig. 3(b).

The interpretation of the structures S_1 – S_3 as surface states is based on the invariance of their dispersions with photon energy and the fact that their energies lie outside the 1×1 projected band structure. Such an interpretation is further supported by comparisons with photoemission spectra obtained from the clean and H-terminated Si(100) 2×1 surfaces. The latter surface provides clear information on the bulk contribution to the Si(100) spectra.

The surface band S_1 does not show any measurable dispersion in the outer half of the 2×2 surface Brillouin zone (SBZ). This is in good agreement with the very weak downward dispersion obtained in the calculation. The experimental dispersion close to Γ is somewhat uncertain since two structures are observed in the 21.2-eV spectra. The structure observed at -1.2 eV at Γ appear as a strong peak while the structure at -0.75 eV appears as a weak shoulder. Based on the variation in intensity of these structures with increasing emission angle, an upward dispersion of S_1 from -1.2 eV at Γ to -0.9 eV at K

is the best interpretation. Close to Γ_2 only the upper of these two structures is observed, but the intensity is very weak. The structures S_2 and S_3 appear as peaks in the spectra between the Γ_2 and K points and exhibit upward dispersion along $\Gamma_2 \rightarrow K$. Each of the three bands observed experimentally has a theoretical counterpart and the correspondence between theory and experiment is very good. All three bands may be classified as In-Si backbond states resulting from interaction of the Si dangling bonds with In p orbitals.

In summary, we have shown that the parallel ad-dimer model has a significantly lower surface energy than the orthogonal ad-dimer model. The surface-state dispersions calculated for the parallel ad-dimer model are in good agreement with the present angle-resolved photoemission data for Si(100) 2×2 :In. Based on calculations of the interaction energy between ad-dimer rows we propose that the 3×2 and 5×2 phases result from repulsive interactions between ad-dimer rows.

The theoretical work was supported in part by ONR Contract No. N00014-82-C0244. The experimental work was supported by the Swedish Natural Science Research Council.

-
- ¹T. Sakamoto and H. Kawanami, *Surf. Sci.* **111**, 177 (1981).
²B. Bourguignon, K. L. Carleton, and S. R. Leone, *Surf. Sci.* **204**, 455 (1988).
³T. Ide, T. Nishimori, and T. Ichinokawa, *Surf. Sci.* **209**, 335 (1989).
⁴J. Nogami, Sang-il Park, and C. F. Quate, *Appl. Phys. Lett.* **53**, 2086 (1988).
⁵A. A. Baski, J. Nogami, and C. F. Quate, *J. Vac. Sci. Technol. A* **8**, 245 (1990).
⁶A. A. Baski, J. Nogami, and C. F. Quate, *J. Vac. Sci. Technol. A* **9**, 1946 (1991).
⁷J. Nogami, A. A. Baski, and C. F. Quate, *Phys. Rev. B* **44**, 1415 (1991).
⁸A. A. Baski, J. Nogami, and C. F. Quate, *Phys. Rev. B* **43**, 9316 (1991).
⁹J. Ihm, A. Zunger, and M. L. Cohen, *J. Phys. C* **12**, 4409 (1979).
¹⁰M. T. Yin and Marvin L. Cohen, *Phys. Rev. B* **26**, 5668 (1982).
¹¹W. Kohn and L. Sham, *Phys. Rev.* **140**, A1135 (1965).
¹²Giovanni B. Bachelet and M. Schluter, *Phys. Rev. B* **25**, 2103 (1982).
¹³Inder P. Batra, *Phys. Rev. Lett.* **63**, 1704 (1989).
¹⁴The radius of a hemispherical Ga cluster having a nucleation barrier of 0.05 eV/atom is ~ 50 Å.
¹⁵F. H. Stillinger and T. A. Weber, *Phys. Rev. B* **31**, 5262 (1985).
¹⁶T. W. Poon, S. Yip, P. S. Ho, and F. F. Abraham, *Phys. Rev. Lett.* **65**, 2161 (1990).
¹⁷E. Pehlke and J. Tersoff, *Phys. Rev. Lett.* **67**, 465 (1991).
¹⁸L. S. O. Johansson, R. I. G. Uhrberg, P. Martensson, and G. V. Hansson, *Phys. Rev. B* **42**, 1305 (1990).
¹⁹A. Ishizaka and Y. Shiraki, *J. Electrochem. Soc.* **133**, 666 (1986).